Fluorine-enhanced Room-temperature Luminescence of Er-doped Crystalline Silicon

Xiaoming Wang[1], Jiajing He[1,2,3*], Shenbao Jin[4], Huan Liu[1], Hongkai Li[5], Huimin Wen[1], Xingyan Zhao[1], Roozbeh Abedini-Nassab[6], Gang Sha[4], Fangyu Yue[5] and Yaping Dan[1*]

[1] University of Michigan-Shanghai Jiao Tong University Joint Institute, Shanghai Jiao Tong University, Shanghai, 200240, China.

[2]Laboratory of Micro-Nano Optoelectronic Materials and Devices, Shanghai Institute of Optics and Fine Mechanics, Chinese Academy of Sciences, Shanghai 201800, China.

[3]CAS Center for Excellence in Ultra-intense Laser Science
Shanghai 201800, China

[4] School of Materials Science and Engineering, Herbert Gleiter Institute of Nanoscience, Nanjing University of Science and Technology, Nanjing, 210094, China.

[5] Key Laboratory of Polar Materials and Devices, Ministry of Education, East China Normal University, Shanghai, 200241, China.

[6]Faculty of Mechanical Engineering, Tarbiat Modares University, Tehran, Iran, P. O. Box: 14115-111

*Email: yaping.dan@sjtu.edu.cn; jiajinghe@sjtu.edu.cn

Author Manuscript

Abstract

The silicon-based light-emitting devices are the bottleneck of fully integrated silicon photonics. Doping silicon with erbium (often along with oxygen) is an attractive approach to turn silicon into a luminescent material, which has been explored for decades. One of the main challenges is the strong thermal quenching effect that results in weak photoluminescence efficiency. Here we show that the co-doping of fluorine with erbium ions can significantly suppress the thermal quenching effect and Auger recombination, resulting in a 3-order-of-magnitude increase in photoluminescence compared to Er/O doped crystalline silicon. As a result, relatively strong photoluminescence is observed from fluorine-doped silicon at room temperature.

Introduction

Silicon photonics will speed up the computing and data transmission of the current communication network by integrating optical and electronic devices on the same silicon substrate.[1-4] This technology requires efficient silicon-based light sources and optical amplifiers at communication wavelengths.[4-6] However, silicon is an indirect band gap semiconductor, which cannot efficiently emit light at communication wavelengths. In the past several decades, significant efforts have been devoted to developing efficient silicon-based light-emitting materials, including III-V quantum dots and strained Ge, epitaxially grown on silicon.[7-12] Doping silicon with erbium ions is the earliest effort to create luminescent silicon, which is also one of the most attractive approaches[13-14] as it is compatible with complementary metal-oxide-semiconductor (CMOS) processes. However, it suffers from strong

This is the author manuscript accepted for publication and has undergone full peer review but has not been through the copyediting, typesetting, pagination and proofreading process, which may lead to differences between this version and the Version of Record. Please cite this article as doi: 10.1002/adpr.202200115.

This article is protected by copyright. All rights reserved

thermal quenching in photoluminescence (PL), resulting in an extremely low efficiency at room temperature (RT).[14-18] Interestingly, our group[19] recently found that the thermal quenching effect can be suppressed by employing a deep cooling process to treat the Er/O co-doped crystalline silicon, as a result of which the PL efficiency at RT is improved by two orders of magnitude. The improvement is due to the fact that the deep cooling process can mitigate the precipitation of erbium ions into Er-O-Si nanocrystals that often occurs in the slow cooling process of standard rapid thermal annealing (RTA). Without the Er/O precipitation into large nanocrystals, the non-radiative emission paths through the interface states between nanocrystalline precipitates and silicon crystal are thus eliminated, resulting in a weak thermal quenching effect in PL. In this work, we surprisingly found that the thermal quenching effect can also be suppressed by co-doping fluorine (F) ions with erbium ions, although Er/F ions have precipitated into large nanocrystals with the standard RTA treatment. It is likely because F ions can passivate the interface states between erbium nanocrystals and Si lattice.

Results and discussion

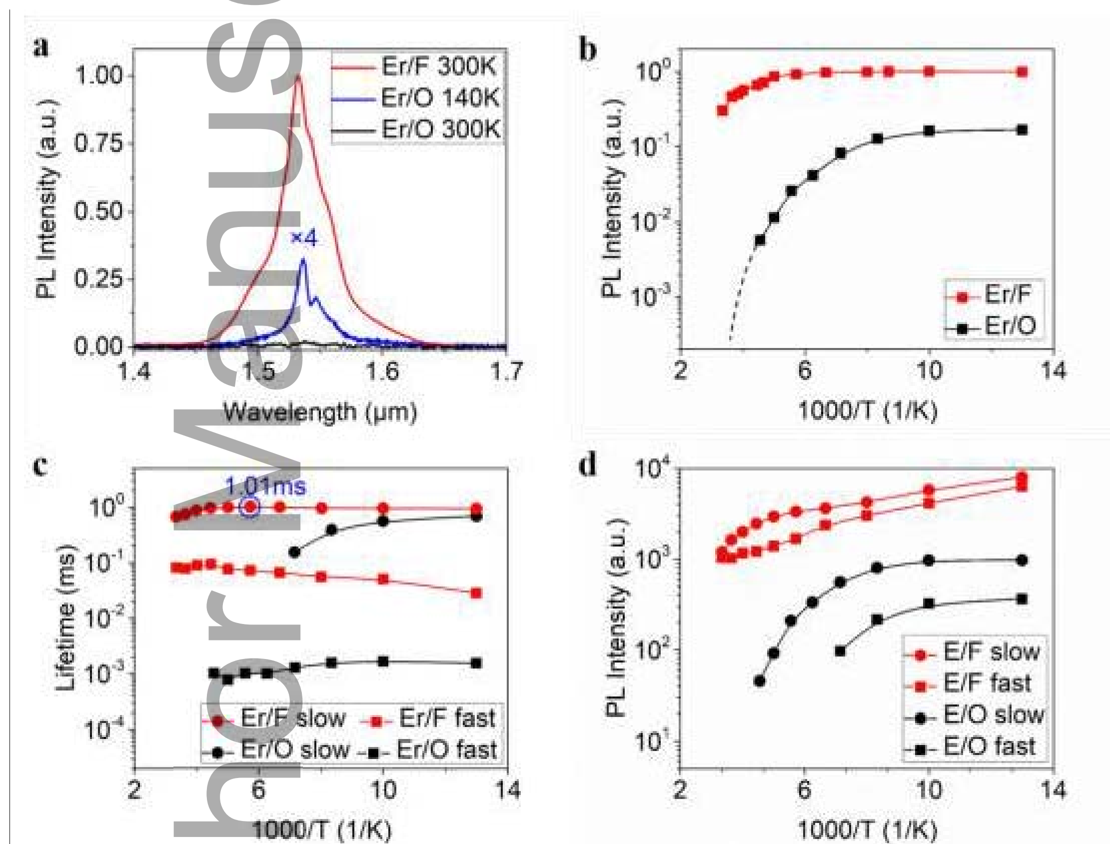

Figure 1. Temperature-dependent steady and transient analysis for Er/F-doped Si and Er/O-doped Si samples. (a) PL spectra of Er/F-Si and Er/O-Si at different temperatures. **(b)** Steady-state PL intensity. **(c)** Fast and slow lifetimes of carriers for Er-doped Si with F (red) and O (black), respectively. The excitation laser was at 405 nm with a power of 200 mW. **(d)** PL intensity of the fast and slow component for the Er/O: Si and Er/F: Si samples.

The intrinsic <100> single crystalline silicon (FZ) wafer was first cleaned with acetone and deionized water, piranha solution (sulfuric acid: 30% hydrogen peroxide=3:1) followed for 20 mins at 100 °C, and rinsed in deionized water. O and F ions were implanted separately into different samples with a dose of 1×10^{16} cm^{-2} at 30 keV to create Er/O and Er/F samples for comparison. Erbium ions were implanted with a dose of 4×10^{15} cm^{-2} at 200 keV. After the implantation, the samples were cut into small pieces and went through the cleaning procedure again. RTA process (900 °C for 5 mins) was applied to activate the implanted atoms and repair the lattice damage caused by ion implantation.

This article is protected by copyright. All rights reserved

PL spectra and decay curves of the Er/F: Si sample excited by a blue laser with a diameter of 1.5 mm (λ=405 nm) were recorded at different temperatures to investigate the thermal quenching effect and the back-transfer dynamics. For comparison, the Er/O: Si sample was also measured since the Er/O: Si samples are the most widely studied. As shown in Figure 1a, no PL is observed in the Er/O: Si samples at RT. For the Er/F: Si sample, the PL spectrum peaked at 1532 nm with a full width half maximum (FWHM) of 40 nm is acquired at RT, as shown in Figure 1a. The PL peak of the Er/F samples is blue-shifted and broadened, likely because the local environment of Er ions is changed by binding with F instead of O. As known, for the Er-doped silicon, strong thermal quenching is one of the main factors that result in the low RT luminescence efficiency. As shown previously, Er-O-Si composites will precipitate as nanocrystals in the crystalline silicon. The lattice mismatch between the nanocrystals and crystalline Si will create a high concentration of interface defects, resulting in strong nonradiative recombination, which can be suppressed at low temperatures[13]. For this reason, it is not surprising that the PL intensity of Er/O doped Si is quenched by more than 3 orders of magnitude as the temperature increases from 77 K to 300 K (Figure 1b), which is widely observed in literatures.[17-18, 20] Surprisingly, the Er/F: Si sample treated by the same RTA process exhibits strong PL emission which is nearly independent of temperature, shown as the red squares in Figure 1b (only quenched by 3 times from 77 K to 300 K). In addition, the Er/F: Si sample exhibits a stronger low temperature PL intensity by one order of magnitude than the Er/O: Si sample. It is likely because the Er/F: Si sample has a higher Er optical activation rate. Clearly, F dopants play an important role that is completely different from O dopants.

To better understand the role of F ions, transient PL decay curves at the peak wavelength were recorded at a pump power of 200 mW as the temperature was lowered from RT to 77 K (s S1, Supporting Information). The PL decay traces for both Er/F and Er/O samples can be well described with a double exponential function as below (eq.1),

$$I(t) = I_{fast}e^{-\frac{t}{\tau_{fast}}} + I_{slow}e^{-\frac{t}{\tau_{slow}}} \quad (1)$$

where τ_{fast} and τ_{slow} are decay times for the fast and slow components, respectively. I_{fast} and I_{slow} are the corresponding fractional contribution. The non-exponential decay behavior suggests at least two relax/recombination channels related to Er states. The extracted lifetimes and PL intensities were shown in Figures 1c and 1d, respectively. For the Er/O: Si sample, τ_{fast} is quite short (~1 μs), two orders of magnitude fast than the general lifetime of Er ion luminescence, which could be related to the non-recombination process, e.g., the fast relaxation or back-transfer to the lower or higher energy levels, or even the Auger recombination. However, τ_{slow}, which is highly dependent on temperature and decreases from 690 to 155 μs when the temperature goes up from 77 K to 140 K, could be related to the lifetime of carriers related to the Er ion luminescence. In contrast, the lifetimes of the Er/F: Si are much larger and nearly independent of temperature. The slow and fast time constant is ~1 ms and 30 ~ 100 μs, respectively.

The radiative recombination lifetimes for Er/O: Si and Er/F: Si samples are the same, since the electronic transition occurs in the inner orbitals of Er ions which are less affected by environment. The PL intensity is proportional to the excited Er concentration. The weak RT PL for the Er/O doped silicon is attributed to a number of factors, including the low concentration of optical active Er, high concentration of non-radiative recombination centers and strong temperature quenching for carrier lifetime.[13, 21-24] In contrast, Er/F doped samples have a much stronger PL which comes along with longer lifetimes and weaker dependence on temperature. In addition, both fast and slow carrier lifetimes exhibit an anomalous temperature dependence. As the temperature goes up, the lifetime of the slow decay component increases, reaching the maximum value of ~1 ms at 175 K. Similar behaviors have been reported and ascribed to the carriers delocalizing from trap states or defect states to excited states and Auger effect is weak.[25-26] It only decays by 3 times with temperature increasing from 77 K to 300 K. The incorporation of F ions increases the intensity of fast and slow components by at least one order of magnitude (Figure 1d). Thermal quenching can be effectively reduced, which means the probability of back transfer is decreased.

This article is protected by copyright. All rights reserved

Author Manuscript

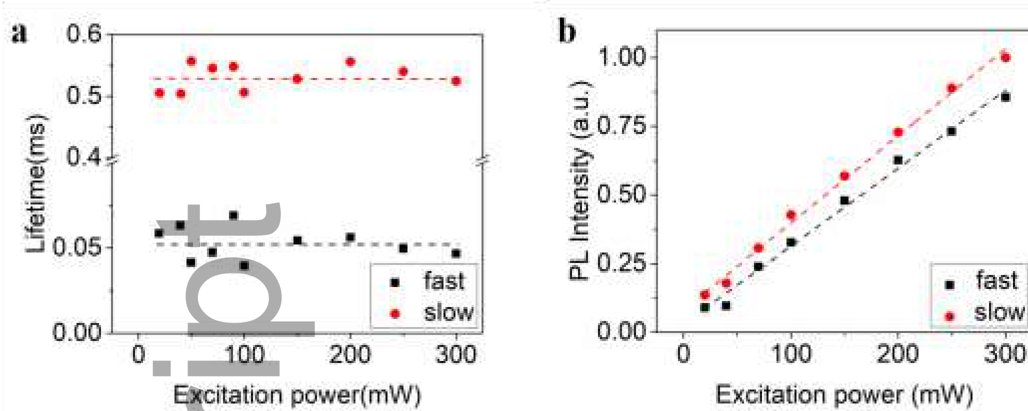

Figure 2. Power-dependent transient analysis for the Er/F: Si sample at 300K. (a) Excitation-dependent fast and slow decay times. **(b)** Excitation-dependent PL intensity of fast and slow components, respectively.

Another factor that limits the PL intensity is the Auger effect and non-radiative recombination via defects. Electrical measurements show that Er/O: Si samples have much lower sheet resistances than the Er/F: Si ones, indicating a high concentration of free electrons in the former. Therefore, Er/O: Si samples will have stronger Auger recombination at high injection. Indeed, for the Er/F: Si sample, Auger effect is negligible, because the lifetimes for the Er/F: Si sample are almost independent of the excitation power as shown in Figure 2a. As a result, the PL intensity of these two components is almost linearly with the pumping power changing within about two orders of magnitude (Figure 2b). It is not difficult to conclude that the incorporation with F, in comparison with co-doped with O, can efficiently suppress the Auger effect and non-radiative recombination via defects.

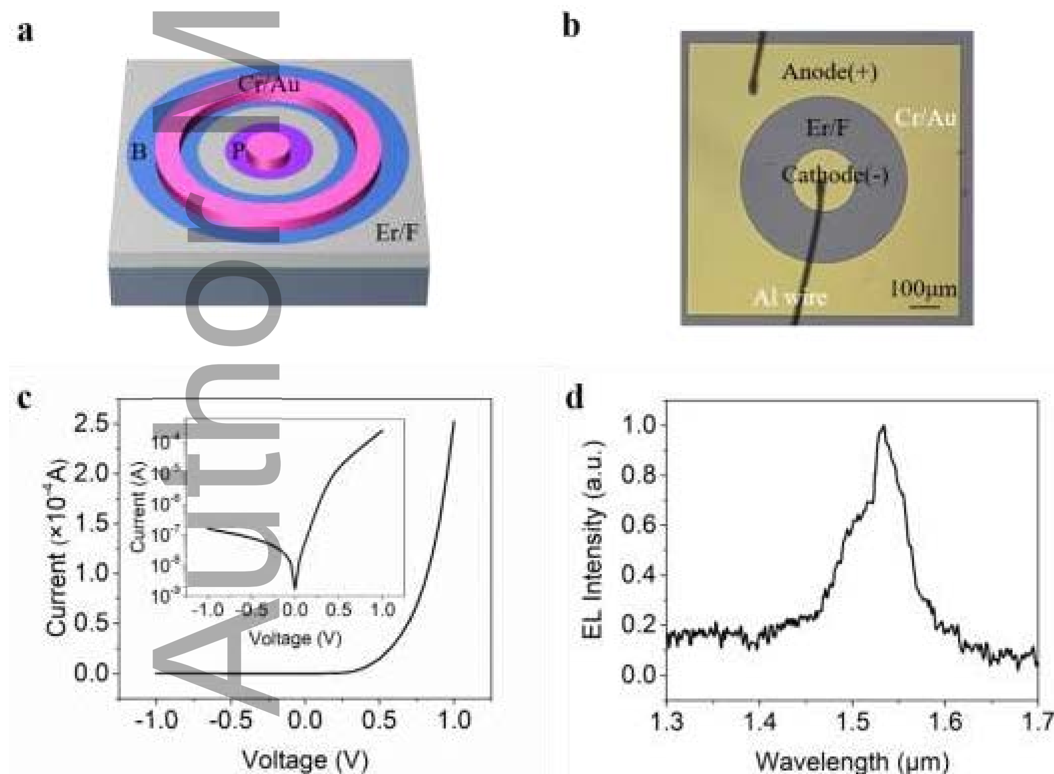

Figure 3. Er/F: Si LED device. (a) 3D structure of the device. **(b)** Schematic of the device. **(c)** I-V curve. Inset: logarithm current vs bias. **(d)** RT EL spectrum.

The Er/F: Si sample was further fabricated into a light-emitting diode (LED). The sheet resistance of Er/F: Si is

Author Manuscript

This article is protected by copyright. All rights reserved

7.3 kΩ/sq. Thus, boron (blue region) and phosphorus (purple region) were implanted to form the p-type and n-type region with a dosage of 1×10^{15} cm^{-2} at 20 keV and 1×10^{14} cm^{-2} at 60 keV, respectively (Figure 3a). The RTA process was employed to activate the dopants at the same time. A pair of co-axial metal electrode patterns were defined, followed by thermal evaporation of 5 nm Cr and 70 nm Au (Optical microscopic image of the device is shown in Figure 3b). The I-V curve exhibits a rectifying behavior of a typical PN junction diode with an on/off ratio of ~ 3 orders of magnitude (Figure 3c). The ideal factor can be calculated as ~2, indicating that a high-quality PN junction diode is made and that electrons from the n^+ region and holes from the p^+ region dominantly recombine within the depletion region. The EL spectrum was measured by a cooled Ge detector with a peak of 1534 nm under the pulse operation condition, as shown in Figure 3d.

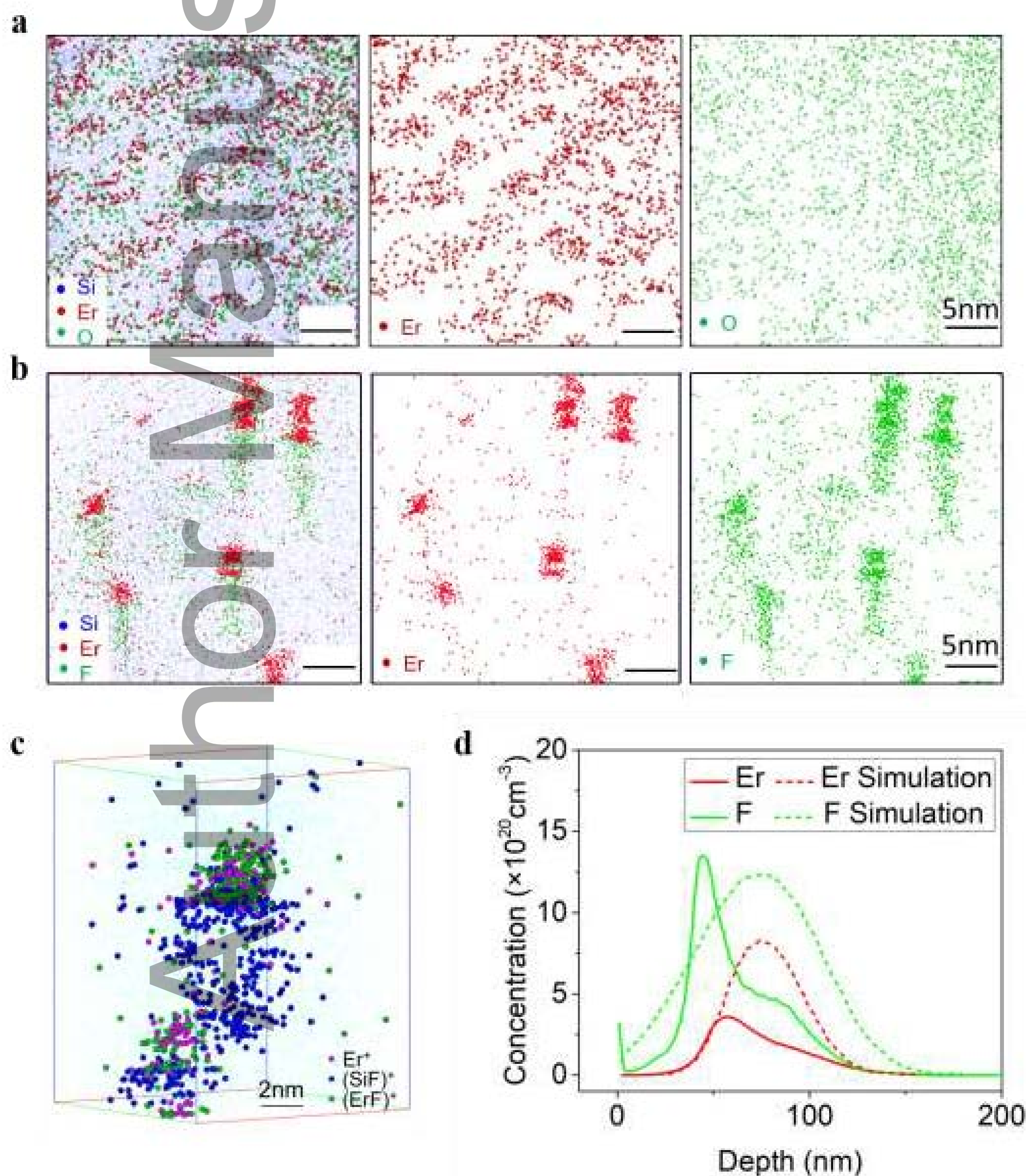

Figure 4. APT characteristic. (a) The spatial distribution of Er and O atoms in the Er/O: Si sample treated by RTA. (b) The spatial distribution of Er and F atoms in the Er/F: Si sample treated by RTA. (c) Three-dimensional

This article is protected by copyright. All rights reserved

Author Manuscript

reconstruction volume with aggregations in the Er/F: Si sample. $(SiF)^+$ refers to SiF and SiF_2. $(ErF)^+$ refers to ErF and ErF_2. (d) SIMS characterization of the RAT treated Er/F: Si sample. Ion distribution profiles of experimental results (solid line) and comparing them to simulation results (dashed lines).

To better understand the luminescence mechanism, APT was used to map the spatial distribution of elements for both Er/O: Si and Er/F: Si samples. For the Er/O: Si sample, Er ions are clearly aggregated into "stripes" while O atoms are more uniformly distributed (Figure 4a). In contrast, both Er and F ions in the Er/F sample precipitate into clusters (Figure 4b). Three-dimensional reconstruction volume of Er and F atoms in Er/F: Si sample is shown in Figure S2 (SI). A closer look at one of the clusters (Figure 4c) indicates that F atoms form larger clusters, wrapping around Er precipitates in the form of Er-F composites. This picture is largely consistent with the fact that F ions likely play a passivation role which leads to a weak thermal quenching effect and a low dark current of the fabricated PN junction.[27-28]

The Er and F atom distribution profiles of the Er/F: Si sample treated by RTA acquired by secondary ion mass spectroscopy (SIMS) are shown in Figure 4d. Compared with the calculated results, the peak positions of Er and F both shift towards the surface of Si, consistent with the fact that Er-F complexes are formed after annealing.[29-30] This observation is in line with previous reports[31-32] that F atoms migrate toward the surface at a temperature beyond 550°C.

Conclusion

We have demonstrated that F has a passivation effect and can enhance the PL of Er-doped Si. In comparison with O dopants, F ions are more mobile and tend to aggregate with Er, potentially passivating defects on the surface of Er precipitates. As a result, the non-radiative recombinations including phonon-assisted relaxation and the Auger effect are suppressed. Unfortunately, the quantum efficiency of the Er/F: Si device is still relatively low due to the low activation rate of Er ions which we plan to improve in the future by exploring novel methods.

Acknowledgement

X.M.W, and J.J.H contributed equally to this work. This work was supported by the "Innovative Research Plan," Shanghai Municipality Bureau of Education (2019-01-07-0002-E00075), China National Postdoctoral Program for Innovative Talents (BX20200205), the National Science Foundation of China (61904102). SB.J. and G.S. would like to acknowledge facility use and scientific and technical assistance from the Materials Characterization Facility in Nanjing University of Science and Technology. The authors are grateful to the support for PL analysis by Dr. Ruibin Wang at Instrumental Analysis Center of Shanghai Jiao Tong University. The devices were fabricated at the Center of Advanced Electronic Materials and Devices (AEMD) Shanghai Jiao Tong University.

Data Availability Statement

The data that support the findings of this study are available from the corresponding author upon reasonable request.

References

[1] A. H. Atabaki, S. Moazeni, F. Pavanello, H. Gevorgyan, J. Notaros, L. Alloatti, M. T. Wade, C. Sun, S. A. Kruger, H. Meng, K. Al Qubaisi, I. Wang, B. Zhang, A. Khilo, C. V. Baiocco, M. A. Popovic, V. M. Stojanovic, R. J. Ram, *Nature* **2018**, 556, 349.

[2] R. Won, *Nature Photonics* **2010**, 4, 498.

This article is protected by copyright. All rights reserved

Author Manuscript

[3] H. Subbaraman, X. Xu, A. Hosseini, X. Zhang, Y. Zhang, D. Kwong, R. T. Chen, *Opt Express* **2015**, 23, 2487.
[4] R. A. Soref, *Proceedings of the IEEE* **1993**, 81, 1687.
[5] R. Soref, *Advances in Optical Technologies* **2008**, 2008, 1.
[6] T. Wang, J.-J. Zhang, L. Huiyun, *Acta Physica Sinica* **2015**, 64.
[7] S. Takagi, R. Zhang, J. Suh, S.-H. Kim, M. Yokoyama, K. Nishi, M. Takenaka, *Japanese Journal of Applied Physics* **2015**, 54.
[8] Y. B. Bolkhovityanov, O. P. Pchelyakov, *Physics-Uspekhi* **2008**, 51, 437.
[9] T. Komljenovic, M. Davenport, J. Hulme, A. Y. Liu, C. T. Santis, A. Spott, S. Srinivasan, E. J. Stanton, C. Zhang, J. E. Bowers, *Journal of Lightwave Technology* **2016**, 34, 20.
[10] F. A. W. Koch B R, Cohen *Optics express* **2007**, 15, 11225.
[11] R. E. Camacho-Aguilera, Y. Cai, N. Patel, J. T. Bessette, M. Romagnoli, L. C. Kimerling, J. Michel, *Optics express* **2012**, 20, 11316.
[12] Z. Zhou, B. Yin, J. Michel, *Light: Science & Applications* **2015**, 4, e358.
[13] A. J. Kenyon, *Semiconductor Science and Technology* **2005**, 20, R65.
[14] A. Polman, *Journal of applied physics* **1997**, 84, 1.
[15] H. Ennen, G. Pomrenke, A. Axmann, K. Eisele, W. Haydl, J. Schneider, *Applied Physics Letters* **1985**, 46, 381.
[16] H. Ennen, J. Schneider, G. Pomrenke, A. Axmann, *Applied Physics Letters* **1983**, 43, 943.
[17] M. A. Lourenco, M. M. Milosevic, A. Gorin, R. M. Gwilliam, K. P. Homewood, *Sci Rep* **2016**, 5, 37501.
[18] F. Priolo, G. Franzò, S. Coffa, A. Carnera, *Physical Review B* **1998**, 57, 4443.
[19] H. Wen, J. He, J. Hong, S. Jin, Z. Xu, H. Zhu, J. Liu, G. Sha, F. Yue, Y. Dan, *Advanced Optical Materials* **2020**, 8.
[20] J. Michel, J. L. Benton, R. F. Ferrante, D. C. Jacobson, D. J. Eaglesham, E. A. Fitzgerald, Y. H. Xie, J. M. Poate, L. C. Kimerling, *Journal of Applied Physics* **1991**, 70, 2672.
[21] D. Eaglesham, J. Michel, E. Fitzgerald, D. Jacobson, J. Poate, J. Benton, A. Polman, Y. H. Xie, L. Kimerling, *Applied Physics Letters* **1991**, 58, 2797.
[22] H. Efeoglu, J. Evans, T. Jackman, B. Hamilton, D. Houghton, J. Langer, A. Peaker, D. Perovic, I. Poole, N. Ravel, *Semiconductor science and technology* **1993**, 8, 236.
[23] G. Van den Hoven, J. H. Shin, A. Polman, S. Lombardo, S. Campisano, *Journal of applied physics* **1995**, 78, 2642.
[24] F. Priolo, G. Franzò, S. Coffa, A. Polman, S. Libertino, R. Barklie, D. Carey, *Journal of Applied Physics* **1995**, 78, 3874.
[25] X. H. Zhang, S. J. Chua, A. M. Yong, H. Y. Yang, S. P. Lau, S. F. Yu, X. W. Sun, L. Miao, M. Tanemura, S. Tanemura, *Applied Physics Letters* **2007**, 90.
[26] B. Ghosh, M. Takeguchi, J. Nakamura, Y. Nemoto, T. Hamaoka, S. Chandra, N. Shirahata, *Sci Rep* **2016**, 6, 36951.
[27] H. C. Sio, D. Kang, R. Liu, J. Stuckelberger, C. Samundsett, D. Macdonald, *ACS Appl Mater Interfaces* **2021**, 13, 32503.
[28] Y. Liu, M. R. Halfmoon, C. A. Rittenhouse, S. Wang, *Applied Physics Letters* **2010**, 97.
[29] F. Ren, J. Michel, D. Jacobson, J. Poate, L. Kimerling, *MRS Online Proceedings Library (OPL)* **1993**, 316.
[30] P. Liu, J. P. Zhang, R. J. Wilson, G. Curello, S. S. Rao, P. L. F. Hemment, *Applied Physics Letters* **1995**, 66, 3158.
[31] X. D. Pi, C. P. Burrows, P. G. Coleman, *Phys Rev Lett* **2003**, 90, 155901.
[32] S. P. Jeng, T. P. Ma, R. Canteri, M. Anderle, G. W. Rubloff, *Applied Physics Letters* **1992**, 61, 1310.

The co-doping of fluorine with erbium ions significantly suppresses the thermal quenching effect and Auger recombination, resulting in a 3-order-of-magnitude increase in photoluminescence compared to Er/O-doped crystalline silicon and relatively strong photoluminescence at room temperature. Since F ions are more mobile and

Author Manuscript

This article is protected by copyright. All rights reserved

tend to aggregate with Er, potentially passivating defects on the surface of Er precipitates.

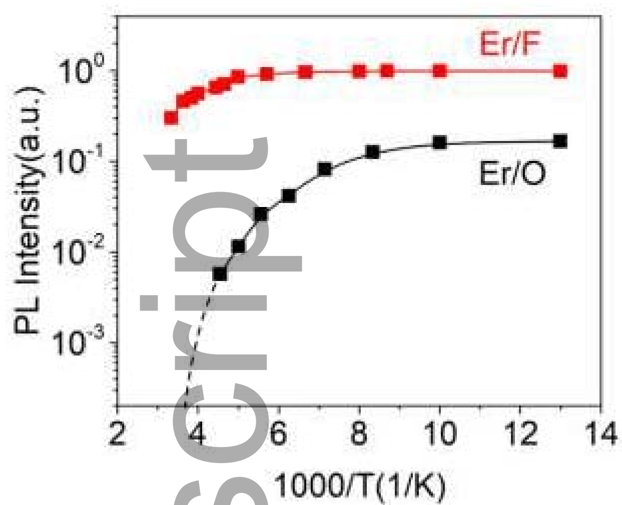

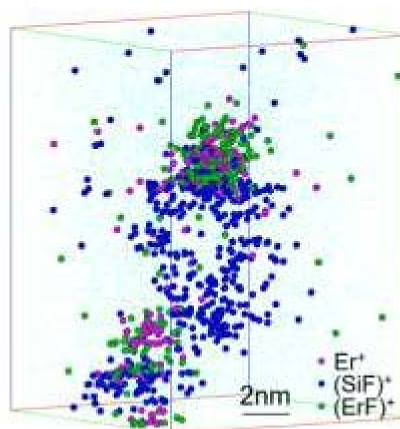

Author Manuscript

This article is protected by copyright. All rights reserved